Bioorganic & Medicinal Chemistry Letters 30 (2020) 127519

Contents lists available at ScienceDirect

Bioorganic & Medicinal Chemistry Letters

journal homepage: www.elsevier.com/locate/bmcl

Novel carboxylated pyrroline-2-one derivatives bearing a phenylhydrazine moiety: Design, synthesis, antifungal evaluation and 3D-QSAR analysis

Min Chen[a], Lizhi Zhang[a,b], Aimin Lu[a], Xiaobin Wang[a], Weijie Si[a], Jinghua Yan[a], Chunlong Yang[a,*]

[a] Jiangsu Key Laboratory of Pesticide Science, College of Sciences, Nanjing Agricultural University, Nanjing, China
[b] Institute of Synthesis, CHIA TAI Tianqing Pharmaceutical Group Co., Ltd, Nanjing, China

ARTICLE INFO

Keywords:
Pyrroline-2-one
Phenylhydrazine
Lead optimization
Antifungal activity
3D-QSAR

ABSTRACT

Aiming to discover novel high-efficient antifungal leads that possess an innovative action mechanism, twenty-three carboxylated pyrroline-2-one derivatives, bearing a phenylhydrazine moiety, were rationally designed and firstly prepared in this letter. The *in vitro* bioassays showed that most of the compounds possessed excellent antifungal effects with the EC_{50} values of less than 1 μg/mL against the phytopathogenic fungi *Fusarium graminearum* (*Fg*), *Botrytis cinerea* (*Bc*), *Rhizoctonia solani* (*Rs*) and *Colletotrichum capsici* (*Cc*). The further bioassays showed that the compound **6u** showed the comparable *in vivo* control effect with carbendazim against fusarium head blight and rice sheath blight. The 3D-QSAR model revealed the pivotal effects of a bulky electron-donating group at the 1-position of pyrrole ring, a bulky electron-withdrawing group at the 4-position of phenyl ring and a small alkyl at the carbonate group on the anti-*Rs* activities of target compounds. The abnormal mycelial morphology and delayed spore germination were observed in the treatments of compound **6u**. Given the excellent and broad-spectrum antifungal effects the target compounds have, we unfeignedly anticipated that the above finding could motivate the discovery of high-efficient antifungal leads, which might possess an innovative action mechanism against phytopathogenic fungi.

The exploding population looming nine billion by 2050 will challenge the world in feeding overfull people with limited arablelands.[1] Without the existing agricultural management practices, especially the wide use of pesticides, crops would face 50% to 82% losses, in which pathogens were responsible for the 8% to 21% losses. Even in the modern using of pesticides, weeds, animal pests and phytopathogenic microorganisms still caused the huge crop losses of at least 10% every year.[2] Concurrently, the heavy use of agrochemicals has brought a series of problems including environmental pollutions, food safeties, pesticide resistances, and so on.[3] Therefore, it is an urgent need for agricultural productions to develop novel pesticide ingredients with efficient, broad-spectrum and eco-friendly features.

Tetramic acids, bearing a unique pyrroline-2-one or pyrrolidine-2,4-dione scaffold, are largely existent in the secondary metabolites that are generated by natural microorganisms.[4,5] For the remarkable bioactivities they displayed, tetramic acids were well reported in the discovery of novel natural products, the synthesis methods, and the screening of pharmacological activities.[6–9] The natural tetramic acids present diverse biological activities, such as herbicidal,[10] antifungal,[11,12] antibacterial,[13,14] antitumor,[15] antiviral,[16] and antioxidative[17] effects. Based on the molecular structures of natural tetramic acids, many pyrroline-2-one or pyrrolidine-2,4-dione derivatives possessing significant antifungal activities were synthesized and documented during the last decades.[18–24] These modified tetramic acids with antifungal bioactivities tend to have two important structural features. To some extent, one molecular characteristic could be concluded as the presence of a bulky polar fragment at the 3-position of the pyrrole skeleton,[18–21] the other is the introduction of a moderate lipophilic moiety into the 4-position of the pyrrole nucleus.[7,22–24]

Hydrazine, not only the important intermediate in the synthesis of the nitrogen heterocyclic ring but also a bioactive group, was usually taken consideration in the optimization of new biological compounds.[25–27] For example, the commercial fungicide famoxadone is the representative compound containing the hydrazine group (Fig. 1).[28] Concurrently, our previous work found that introducing a moderate hydrazine fragment could effectively improve the antifungal effects of synthetic compounds (Fig. 1).[26,29] As another important fragment existing in commercial fungicides, carboxylic ester frequently appears in the lipophilic moieties that effectively regulate the molecular penetrability within living organisms.[30] For instance, the commercial fungicides azoxystrobin and pefurazoate contain the carboxylic ester in their structures (Fig. 1). Meanwhile, our previous work documented that

* Corresponding author.
E-mail address: ycl@njau.edu.cn (C. Yang).

https://doi.org/10.1016/j.bmcl.2020.127519
Received 7 July 2020; Received in revised form 20 August 2020; Accepted 21 August 2020
Available online 27 August 2020
0960-894X/

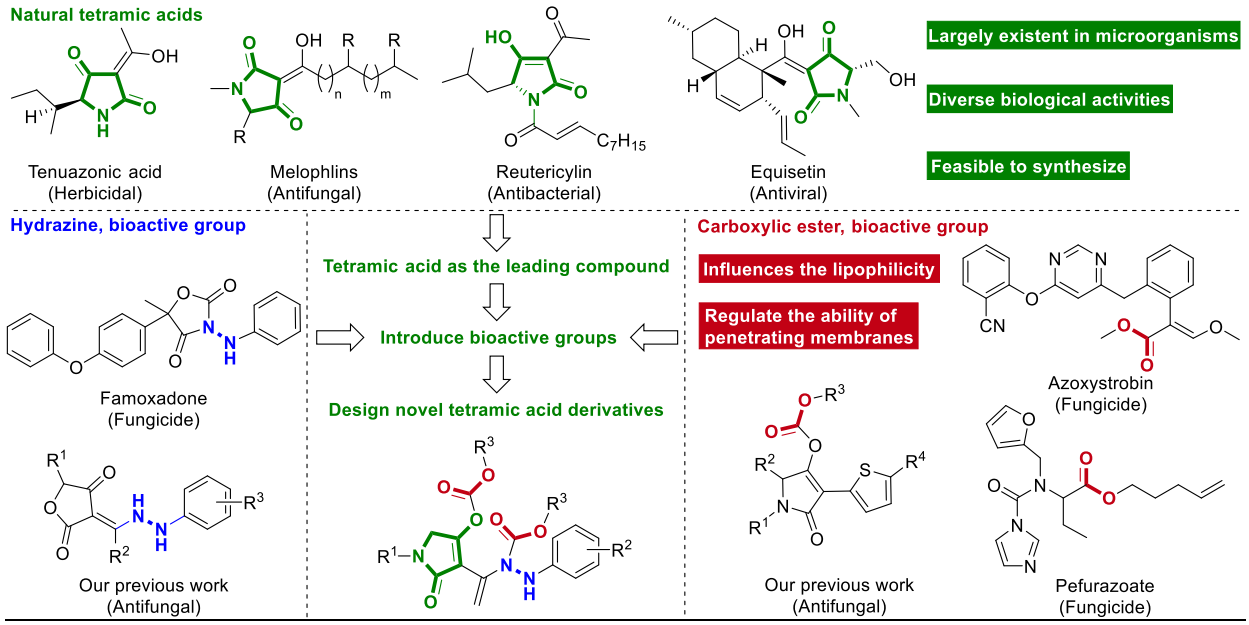

Fig. 1. Design strategy of target tetramic acid derivatives.

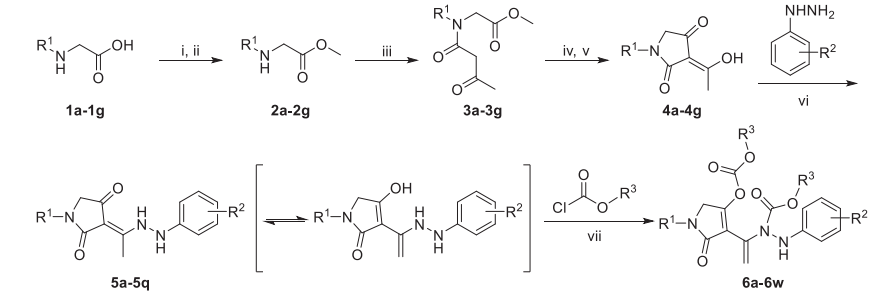

6a: R^1=H, R^2=4-Cl, R^3=Me; **6b**: R^1=H, R^2=4-Cl, R^3=Et; **6c**: R^1=H, R^2=4-Cl, R^3=*n*-Pr; **6d**: R^1=H, R^2=4-Cl, R^3=*i*-Pr;
6e: R^1=H, R^2=4-Cl, R^3=*n*-Bu; **6f**: R^1=H, R^2=4-Cl, R^3=*i*-Bu; **6g**: R^1=H, R^2=4-Cl, R^3=Bn; **6h**: R^1=H, R^2=H, R^3=*i*-Pr;
6i: R^1=H, R^2=4-Me, R^3=*i*-Pr; **6j**: R^1=H, R^2=3,4-di-Me, R^3=*i*-Pr; **6k**: R^1=H, R^2=4-OMe, R^3=*i*-Pr; **6l**: R^1=H, R^2=2-F, R^3=*i*-Pr;
6m: R^1=H, R^2=4-F, R^3=*i*-Pr; **6n**: R^1=H, R^2=2-Cl, R^3=*i*-Pr; **6o**: R^1=H, R^2=3-Cl, R^3=*i*-Pr; **6p**: R^1=H, R^2=2,4-di-Cl, R^3=*i*-Pr;
6q: R^1=H, R^2=4-Br, R^3=*i*-Pr; **6r**: R^1=Me, R^2=4-Cl, R^3=*i*-Pr; **6s**: R^1=Et, R^2=4-Cl, R^3=*i*-Pr; **6t**: R^1=acetyl, R^2=4-Cl, R^3=*i*-Pr;
6u: R^1=cyclopropyl, R^2=4-Cl, R^3=*i*-Pr; **6v**: R^1=cyclohexyl, R^2=4-Cl, R^3=*i*-Pr; **6w**: R^1=Bn, R^2=4-Cl, R^3=*i*-Pr.

Scheme 1. Synthesis route of target compounds **6a-6w**. Reagents and conditions: (i) $SOCl_2$, MeOH, r.t., 1 h then reflux 4 h; (ii) MeONa, MeOH, neutralization; (iii) diketene, r.t., 10 h; (iv) MeONa, MeOH, reflux 4 h; (v) 20% HCl, acidification to pH = 2–3; (vi) Et_3N, EtOH, reflux, TLC monitoring; (vii) Et_3N, $CHCl_3$, 0–4 °C, 30 min.

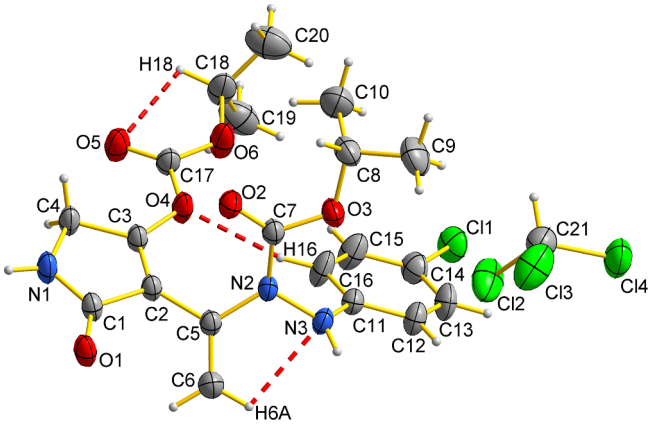

Fig. 2. ORTEP diagram of compound **6d** showing intramolecular hydrogen bonds (red dotted lines).

some bioactive molecules containing a carboxylic ester moiety showed obvious inhibition effects against phytopathogenic fungi.[22,31]

Based on the structural features of tetramic acid derivatives exhibiting antifungal bioactivities, phenylhydrazine, carboxylic ester and carbonate fragments were respectively introduced into the 3- and 4-positions of pyrrole skeleton to tactfully conceive twenty-three novel pyrroline-2-one derivatives (Scheme 1).[21] Using *N*-substituted glycines (**1a–1g**) as raw materials, pyrrolidine-2,4-dione analogues (**4a–4g**) were successfully synthesized by three successive steps including esterification, acylation and cyclization (Scheme 1).[29] Subsequently, substituted phenylhydrazines were introduced into the 3-position of compounds **4a–4g** to prepare the key intermediates pyrrolidine-2,4-diones bearing a phenylhydrazine moiety (**5a–5q**).[30] Finally, the intermediates **5a–5q** reacted with different chloroformates to conveniently generate the target compounds (**6a–6w**) with synthetic yields ranged from 49% to 80% (Table S1 in Supporting information). The structures of all target compounds were confirmed by FT-IR, ^{1}H NMR, ^{13}C NMR and HRMS. The structure of compound **6d** was further confirmed by the single crystal X-ray analysis (Fig. 2).

Table 1
In vitro antifungal EC_{50} values (μg/mL) of target compounds **6a–6w**.[a]

Compound	R^1	R^2	R^3	*Fg*	*Bc*	*Rs*	*Cc*
6a	H	4-Cl	Me	0.71 ± 0.21	0.19 ± 0.04	0.09 ± 0.15	0.55 ± 0.45
6b	H	4-Cl	Et	0.42 ± 0.11	0.14 ± 0.03	0.12 ± 0.13	0.53 ± 0.37
6c	H	4-Cl	*n*-Pr	0.51 ± 0.12	0.20 ± 0.21	0.14 ± 0.21	0.47 ± 0.41
6d	H	4-Cl	*i*-Pr	0.33 ± 0.33	0.18 ± 0.17	0.24 ± 0.23	0.26 ± 0.20
6e	H	4-Cl	*n*-Bu	0.38 ± 0.49	0.22 ± 0.23	0.12 ± 0.19	0.37 ± 0.41
6f	H	4-Cl	*i*-Bu	0.24 ± 0.40	0.23 ± 0.24	0.17 ± 0.24	0.51 ± 0.60
6g	H	4-Cl	Bn	0.30 ± 0.61	0.39 ± 0.38	0.14 ± 0.51	0.54 ± 0.44
6h	H	H	*i*-Pr	1.86 ± 1.76	1.14 ± 1.31	1.67 ± 2.31	1.24 ± 1.04
6i	H	4-Me	*i*-Pr	0.26 ± 0.09	0.35 ± 0.27	1.08 ± 1.32	0.62 ± 2.74
6j	H	3,4-di-Me	*i*-Pr	0.77 ± 0.30	0.58 ± 0.43	2.08 ± 1.54	1.66 ± 1.47
6k	H	4-OMe	*i*-Pr	0.68 ± 1.02	0.67 ± 0.56	1.21 ± 1.38	1.29 ± 0.48
6l	H	2-F	*i*-Pr	66.59 ± 7.92	2.38 ± 1.91	2.23 ± 2.47	1.39 ± 1.53
6m	H	4-F	*i*-Pr	0.31 ± 0.17	0.27 ± 0.28	0.73 ± 0.95	0.29 ± 0.34
6n	H	2-Cl	*i*-Pr	176.33 ± 9.11	3.85 ± 3.02	2.05 ± 2.45	2.07 ± 1.48
6o	H	3-Cl	*i*-Pr	0.80 ± 0.08	0.49 ± 0.51	1.09 ± 1.71	0.53 ± 0.57
6p	H	2,4-di-Cl	*i*-Pr	2.23 ± 2.66	0.65 ± 0.79	0.82 ± 0.67	0.90 ± 0.87
6q	H	4-Br	*i*-Pr	0.22 ± 0.11	0.21 ± 0.33	0.60 ± 0.42	0.31 ± 0.92
6r	Me	4-Cl	*i*-Pr	0.30 ± 0.34	0.16 ± 0.23	0.14 ± 0.29	0.23 ± 1.43
6s	Et	4-Cl	*i*-Pr	0.48 ± 0.11	0.13 ± 0.14	0.07 ± 0.65	0.22 ± 2.87
6t	acetyl	4-Cl	*i*-Pr	0.36 ± 0.34	0.13 ± 0.16	0.23 ± 0.32	0.16 ± 1.02
6u	cyclopropyl	4-Cl	*i*-pr	0.28 ± 0.04	0.11 ± 0.12	0.11 ± 0.16	0.22 ± 0.54
6v	cyclohexyl	4-Cl	*i*-Pr	0.40 ± 0.35	0.26 ± 0.36	0.12 ± 0.31	0.28 ± 0.73
6w	Bn	4-Cl	*i*-Pr	0.39 ± 0.12	0.19 ± 0.31	0.09 ± 0.15	0.29 ± 0.53
Carbendazim	/	/	/	0.49 ± 0.14	/	0.54 ± 0.42	/
Procymidone	/	/	/	/	0.36 ± 0.67	/	/
Validamycin A	/	/	/	/	/	212.15 ± 15.46	/
Azoxystrobin	/	/	/	/	/	/	0.33 ± 0.32

[a] Values are the average of three replicates.

The *in vitro* antifungal activities of compounds **6a–6w** against *Fusarium graminearum* (*Fg*), *Botrytis cinerea* (*Bc*), *Rhizoctonia solani* (*Rs*) and *Colletotrichum capsici* (*Cc*) were assayed at the concentration of 10 μg/mL.[29] As illustrated in Table S4 (Supporting information), all compounds showed remarkable antifungal activities, in which, seventeen compounds exhibited the inhibition rates over 80% against the four phytopathogenic fungi mentioned above. Delightedly, the compounds **6a**, **6c**, **6d**, **6m**, **6q**, **6s**, **6t**, **6u** and **6w** displayed up to 90% inhibitory effects against all tested fungi, and the compounds **6a**, **6b**, **6c**, **6e** and **6f** could completely inhibited the mycelial growth of *Fg*. Thereafter the EC_{50} values of target compounds against the four fungi were tested and presented in Table 1. As shown in Table 1, the anti-*Fg* EC_{50} values of **6b**, **6d–6g**, **6i**, **6m**, **6q–6w** (0.11–0.48 μg/mL) were equivalent or obviously better than that of carbendazim (0.49 μg/mL). For the fungus *Bc*, the compounds **6a–6f**, **6i**, **6m** and **6q–6w** had inhibition effects with the EC_{50} values ranging from 0.11 μg/mL to 0.35 μg/mL, which were better than the control fungicide procymidone (0.36 μg/mL). Meanwhile, the compounds **6d**, **6m** and **6q–6w** exhibited lower anti-*Cc* EC_{50} values (0.16–0.31 μg/mL) than the control fungicide azoxystrobin (0.33 μg/mL). Furthermore, the antifungal EC_{50} values of **6a** (0.09 μg/mL), **6b** (0.12 μg/mL), **6e** (0.12 μg/mL), **6s** (0.07 μg/mL), **6u** (0.11 μg/mL), **6v** (0.12 μg/mL) and **6w** (0.09 μg/mL) against *Rs* were obviously superior to that of carbendazim (0.54 μg/mL) and validamycin A (212.15 μg/mL), which showed remarkable *in vivo* activity against *Rs* and has been widely used in Asia.[32]

The *in vivo* antifungal effects of the compound **6u** against *Rs* and *Fg* were further evaluated, and the corresponding results were vividly presented in Fig. 3–5.[27] As can be seen from Fig. 3, the control efficiency of the compound **6u** against fusarium head blight (FHB) reached 44.7% at 200 μg/mL, which was comparable to that of carbendazim (41.7%). Meanwhile, the compound **6u** showed 45.0% control efficiency against rice sheath blight (RSB) on the rice leaves at 200 μg/mL (Fig. 4) with the referenced comparisons carbendazim (52.8%) and validamycin A (84.7%). Similar with the results observed on rice leaves, the control efficiency of compound **6u** against RSB on rice plants exhibited 69.8% at 200 μg/mL (Fig. 5), whereas carbendazim and validamycin A showed control efficiencies of 82.1% and 91.3%, respectively. All the tested results mentioned above indicate that the compound **6u** had obvious *in vivo* antifungal effects against *Fg* and *Rs*.

Aiming to deeply understand the structure–activity relationships of designed compounds against the fungus *Rs*, a comparative molecular field analysis (CoMFA) was successfully constructed. The calculated statistical parameters relevant to the above CoMFA model are provided in Table S9 (Supporting information).[33] The cross-validated coefficient q^2, optimum number of components, non-cross-validated correlation coefficient r^2, standard error of estimate and *F*-test value were

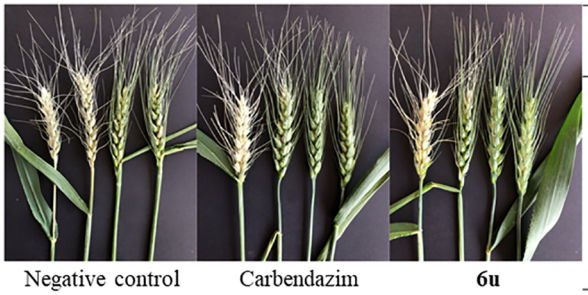

Treatment	Control efficiency (%)
Negative control	–
Carbendazim	41.7±10.7
6u	44.7±8.5

Fig. 3. *In vivo* control efficacy of compound **6u** against *Fg* at 200 μg/mL.

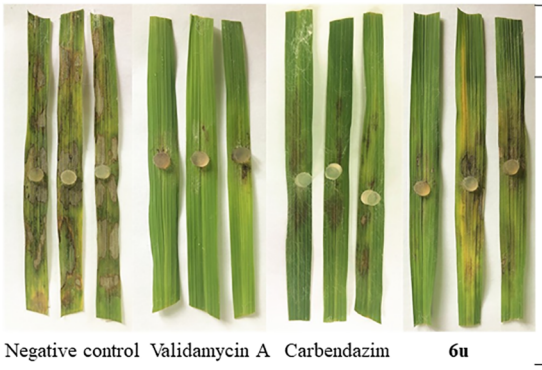

Treatment	Control efficiency (%)
Negative control	–
Validamycin A	84.7±2.6
Carbendazim	52.8±12.3
6u	45.0±11.8

Fig. 4. *In vivo* control efficacy of compound **6u** against *Rs* on rice leaves at 200 μg/mL.

Treatment	Control efficiency (%)
Negative control	–
Validamycin A	91.3±3.0
Carbendazim	82.1±8.3
6u	69.8±9.2

Fig. 5. *In vivo* control efficiency of compound **6u** against *Rs* on rice plants at 200 μg/mL.

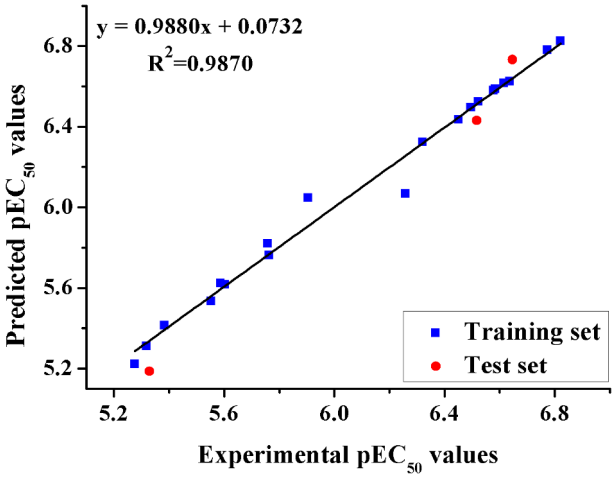

Fig. 6. Correlation between experimental and predicted pEC_{50} values in CoMFA model.

calculated as 0.795, 9, 0.988, 0.081 and 89.687, respectively. The q^2 and r^2 values mentioned above met the validation criterion ($q^2 > 0.5$ and $r^2 > 0.8$), which indicated the generated CoMFA model had good internal predictive ability and reliability. In the CoMFA model, all synthesized compounds were randomly divided into two sections including a training set and a test set (Table S10 in Supporting information). The predicted anti-*Rs* pEC_{50} values predicted by the obtained CoMFA model and the corresponding experimental pEC_{50} values are also summarized in Table S10 (Supporting information), and their correlation is vividly presented in Fig. 6.

In the steric map of CoMFA (Fig. 7A), green blocks, around the 1-position of a pyrrole ring (R^1) and the 4-position of phenyl ring (R^2), indicated that steric bulky substituents in these positions is associated with greater anti-*Rs* activities of target compounds. As predicted by the above model, compounds **6r–6w** bearing alkyl or acetyl substituents at the R^1 position had better EC_{50} values than compound **6d** bearing a hydrogen atom at the R^1 position. Concurrently, the target compounds, bearing substituents at the 4-position of phenyl ring (R^2), exhibited better anti-*Rs* effects than the unsubstituted compound **6h**, no matter the substituted groups were electron-donating (**6i** and **6k**) or electron-withdrawing (**6d**, **6m** and **6q**) groups. The yellow blocks (Fig. 7A), nearby the alkyl section of carbonate group (R^3) and the 2-position of the phenyl ring (R^2), indicated that steric bulky substituents in these positions is associated with worse anti-*Rs* activities. For example, the compounds **6l** and **6n**, bearing substituents at the 2-position of the phenyl ring (R^2), have lower EC_{50} values than the unsubstituted compound **6h**. In the electrostatic map of CoMFA (Fig. 7B), the red and blue blocks meant the electron-withdrawing and electron-donating groups in these regions might increase the anti-*Rs* activity. In fact, both the electron-withdrawing group substituted compounds, such as **6d** (R^2 = 4-Cl), **6m** (R^2 = 4-F) and **6q** (R^2 = 4-Br), as well as the electron-donating group substituted compounds, such as **6i** (R^2 = 4-CH_3) and **6k** (R^2 = 4-OCH_3), had better anti-*Rs* activity than the unsubstituted compound **6h**. However, the compounds **6d**, **6m** and **6q** had better EC_{50} values than the compounds **6i** and **6k**. This reflects the fact that the red blocks were more than blue blocks in number and size near the 4-position of phenyl ring (Fig. 7B). Besides that, a blue block located at the R^1 position reflected the fact that the compounds **6r**, **6s** and **6u–6w** (R^1 = electron-donating groups) had better anti-*Rs* activities than **6d** (R^1 = H) and **6t** (R^1 = acetyl, an electron-withdrawing group).

The effects of compound **6u** against *Fg* and *Rs* on mycelial morphologies were observed by an optical electron microscope and were illustrated in Fig. 8.[34] As shown in Fig. 8A and 8D, the mycelia of

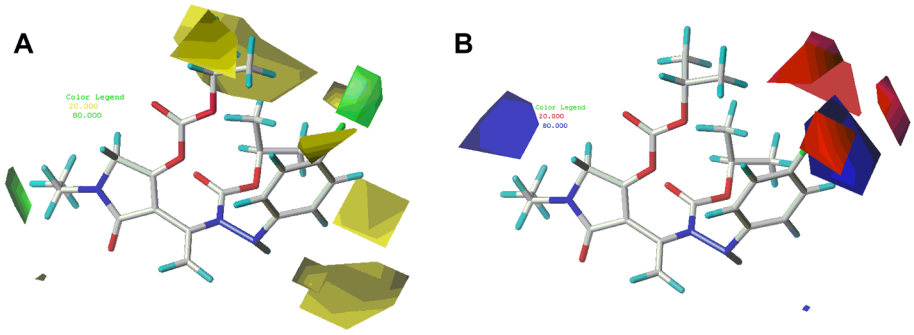

Fig. 7. CoMFA contour maps showing compound **6u**. (A) Steric fields: green and yellow blocks mean steric-bulk favored and steric-bulk disfavored regions, respectively; (B) Electrostatic fields: red blocks mean electron-withdrawing group favored regions and blue blocks represent electron-donating group favored regions.

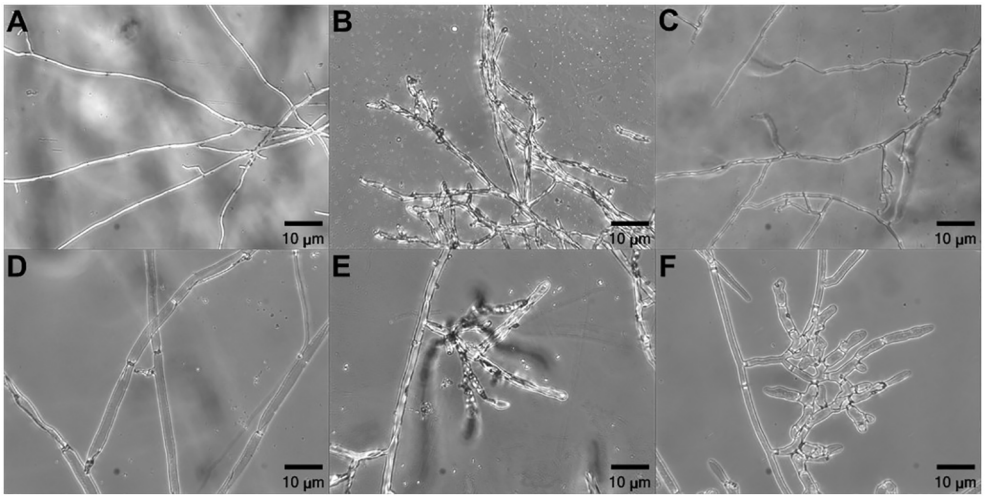

Fig. 8. Mycelial morphology of *Fg* and *Rs* treated with compound **6u**. (A) Negative control of *Fg*; (B and C) *Fg* treated with compound **6u** at 1 μg/mL; (D) Negative control of *Rs*; (E and F) *Rs* treated with compound **6u** at 1 μg/mL.

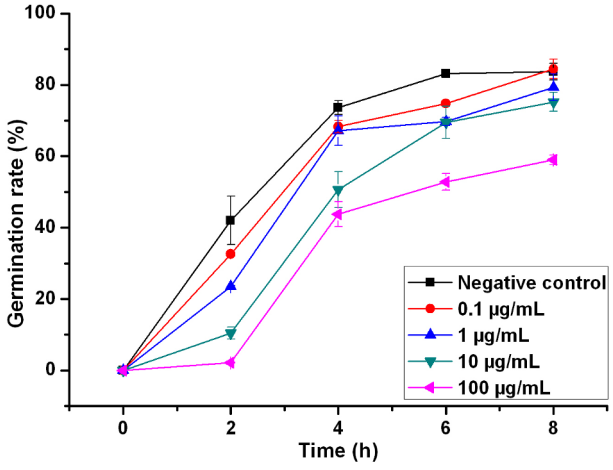

Fig. 9. Influences of compound **6u** on spore germination rates against *Fg*.

both *Fg* and *Rs* in the negative controls were regular and smooth. After treatment by compound **6u** at the concentration of 1 μg/mL, the mycelia showed difference in morphologies compared with the negative control, such as the abnormal hyperplasia at tips (Fig. 8B, 8E and 8F), the shrinkage and collapse of mycelium (Fig. 8C and 8E), and the blurring effects on mycelium outline (Fig. 8B, 8C and 8E). It was obvious that the mycelial growth and the cytoderm integrity of fungus cell were greatly damaged after the treatment with compound **6u**.

The influences of compound **6u** against *Fg* on spore germination were subsequently investigated at different time intervals, and the obtained results were vividly shown in Fig. 9. As shown in Fig. 9, the germination rates of each treatment gradually increased as time goes on. Compared with the negative control, the fungal spores treated with compound **6u** were inhibited in germination rates with the inhibition effects gradually increased over the concentration of compound **6u**. According to the germination curves, we inferred that compound **6u** could delay the germination of *Fg* spores but not completely inhibit.

In summary, a series of novel carboxylated pyrroline-2-one derivatives bearing a phenylhydrazine moiety were rationally designed and firstly prepared. The structures of these synthesized compounds were well characterized using spectroscopic analyses and single crystal X-ray diffraction. Fourteen target compounds showed excellent *in vitro* antifungal effects with the EC_{50} values of less than 1 μg/mL against the tested four pathogenic fungi (*Fg*, *Bc*, *Rs* and *Cc*). The compound **6u** showed the comparable *in vivo* control effect with carbendazim against *Fg* and *Rs*. The constructed 3D-QSAR model revealed that the antifungal activities of target compounds would conducively improve by introducing a bulky electron-donating group at the 1-position of a pyrrole ring (R^1), a bulky electron-withdrawing group at the 4-position of a phenyl ring (R^2) and a small alkyl at the carbonate group (R^3). The abnormal mycelial morphology and delayed spore germination were observed in the treatments of compound **6u**. Given the excellent and broad-spectrum antifungal effects of target compounds that is firstly constructed in our present work, we unfeignedly anticipated that the above finding could motivate the discovery of high-efficient antifungal leads, which possess an innovative action mechanism against phytopathogenic fungi.

Declaration of Competing Interest

The authors declare that they have no known competing financial interests or personal relationships that could have appeared to influence the work reported in this paper.

Acknowledgements

This study was supported by the National Natural Science Foundation of China (31772209) and the Fundamental Research Funds for the Central Universities of China (KYTZ201604 and KJSY201607).

Appendix A. Supplementary data

Supplementary data to this article can be found online at https://doi.org/10.1016/j.bmcl.2020.127519.

References

1. Li D, Zhang S, Song Z, et al. *Eur J Med Chem.* 2017;136:114–121.
2. Epstein L. *Annu Rev Phytopathol.* 2014;52:377–402.
3. Regueiro J, Olguín N, Simal-Gándara J, et al. *Environ Res.* 2015;140:37–44.
4. Royles BJL. *Chem Rev.* 1995;95:1981–2001.
5. Maarisit W, Yamazaki H, Kanno S, et al. *Bioorg Med Chem Lett.* 2017;27:999–1002.
6. Henning HG, Gelbin A. *Adv Heterocycl Chem.* 1993;57:139–185.
7. Wang S, Bao L, Song D, et al. *Eur J Med Chem.* 2019;179:567–575.
8. Kauhl U, Andernach L, Weck S, et al. *J Org Chem.* 2016;81:215–228.
9. Schobert R, Schlenk A. *Bioorg Med Chem.* 2008;16:4203–4221.
10. Zhou B, Wang H, Meng B, et al. *Pest Manag Sci.* 2019;75:2482–2489.
11. Lang G, Blunt JW, Cummings NJ, et al. *J Nat Prod.* 2005;68:810–811.
12. Healy AR, Vinale F, Lorito M, et al. *Org Lett.* 2015;17:692–695.
13. Cherian PT, Cheramie MN, Marreddy RKR, et al. *Bioorg Med Chem Lett.* 2018;28:3105–3112.
14. Matiadis D, Tsironis D, Stefanou V, et al. *Bioorg Med Chem Lett.* 2020;30:127107.
15. Aoki S, Higuchi K, Ye Y, et al. *Tetrahedron.* 2000;56:1833–1836.
16. Sun YL, Wang J, Wang YF, et al. *Tetrahedron.* 2015;71:9328–9332.
17. Hoshino S, Wakimoto T, Zhang H, et al. *Bioorg Med Chem Lett.* 2015;25:3953–3955.
18. Zhu X, Huang L, Wang X, et al. Chin. *J Org Chem.* 2009;29:1784–1789.
19. Wang XF, Si TF, Li QB, et al. *ARKIVOC.* 2010;ii:31–48.
20. Lu GH, Chu HB, Chen M, et al. *Chin Chem Lett.* 2014;25:61–64.
21. Zhang L, Ren Z, Lu A, et al. *Chem Res Chin Univ.* 2015;31:228–234.
22. Xu WQ, Chen M, Wang KY, et al. *Molecules.* 2016;21:355.
23. Wang X, Ren Z, Wang M, et al. *Chem Cent J.* 2018;12:83.
24. Wang X, Ren Z, Mei Y, et al. *J Heterocycl Chem.* 2019;56:165–171.
25. Li LX, Jiao J, Wang XB, et al. *Molecules.* 2018;23:746.
26. Wang X, Fu X, Chen M, et al. *Chin Chem Lett.* 2019;30:1419–1422.
27. Wang X, Dai ZC, Chen YF, et al. *Eur J Med Chem.* 2017;126:171–182.
28. Chrysayi-Tokousbalides M, Kastanias MA, Philippoussis A, et al. *Crop Prot.* 2007;26:469–475.
29. Hu Y, Wang J, Lu A, et al. *Bioorg Med Chem Lett.* 2014;24:3772–3776.
30. Lee CK, Uchida T, Kitagawa K, et al. *J Pharm Sci.* 1994;83:562–565.
31. Wang JJ, Si WJ, Chen M, et al. *J Pestic Sci.* 2017;42:84–92.
32. Chen X, Lu Y, Fan Y, et al. Validamycin and Its Derivatives: Discovery, Chemical Synthesis and Biological Activity. Elseiver, 2017;115–164.
33. Shao WB, Zheng YT, Liu JM, et al. *Bioorg Med Chem Lett.* 2020;30:126912.
34. Qu T, Gao S, Li J, et al. *Pestic Biochem Physiol.* 2017;135:47–51.